2-mercaptobenzothiazole corrosion inhibitor deposited at ultra-low pressure on model copper surfaces

Xiaocui Wu, Frédéric Wiame, Vincent Maurice, Philippe Marcus

2-mercaptobenzothiazole corrosion inhibitor deposited at ultra-low pressure on model copper surfaces

Xiaocui Wu, Frédéric Wiame*, Vincent Maurice, Philippe Marcus*

Université PSL, CNRS - Chimie ParisTech, Institut de Recherche de ChimieParis, Groupe Physico-Chimie des Surfaces, 75005 Paris, France

Abstract

Adsorption of 2-mercaptobenzothiazole (2-MBT) at ultra-low pressure and room temperature on metallic and pre-oxidized Cu(111) surfaces and its thermal stability were investigated using X-ray photoelectron spectroscopy in order to better understand the interfacial corrosion inhibiting properties. 2-MBT is lying flat in the monolayer with two sulphur atoms bonded to Cu and decomposes partially yielding atomic sulphur when interacting with metallic copper prior to forming molecular multilayers. Decomposition is prevented by surface pre-oxidation with 2D oxide dissociation accelerating the 2-MBT initial adsorption kinetics. 2-MBT further decomposes and partially desorbs above 100°C. A pre-adsorbed 2-MBT monolayer on metallic copper inhibits surface corrosion.

Keywords: A. 2-MBT, A. Copper, C. Corrosion inhibition, B. XPS

1. Introduction

Copper is widely used in various applications for its excellent thermal and electrical properties, however it is not immune against corrosion. The use of corrosion inhibitors is considered as an effective way to protect copper [1–6]. The most studied compound is benzotriazole [7–18], but there are also other nitrogen and/or sulphur heterocyclic compounds of interest, especially 2-mercaptobenzothiazole (2-MBT) [19–24]. The presence of nitrogen and

*Corresponding authors

Email addresses: frederic.wiame@chimieparistech.psl.eu (Frédéric Wiame), philippe.marcus@chimieparistech.psl.eu (Philippe Marcus)

sulphur in the organic molecule could improve its capacity as corrosion inhibitor by forming coordinative bonds with copper [1]. It has been shown that 2-MBT dissolved in solution can react with copper to form a complex which acts as a protective layer at the copper surface [21]. However, controversy exists on the chemical nature of the complex formed, as well as on the fundamental mechanisms of the inhibiting interaction. The resulting structures of the protective layer formed on copper are also still not clear. Most notably, the exact role of the surface oxide in the inhibiting function remains to be studied.

With few exceptions [12], experimental research concerning corrosion inhibitors have been done by immersion into solutions containing the organic compounds [7–24]. However, in order to elucidate the interaction mechanisms, deposition of the molecule evaporated in vacuum could be more insightful, since it allows controlling each step of the deposition process in a well-defined environment and on a well-defined surface. Data have been reported for vacuum evaporation [25, 26] of 1,4-benzenedimethanethiol (BDMT) on Au(111), Au(110), Cu(100) and Cu(111) single crystal surfaces. The authors found that on Cu(100) and Cu(111) surfaces, which are more reactive, BDMT dissociates in the initial stage of adsorption, resulting in atomic S adsorbed on the Cu surface. This phenomenon was not observed for the adsorption of benzotriazole on Cu(100) [27].

In this work, the adsorption of 2-MBT at ultra-low pressure (ULP) and room temperature on clean and pre-oxidized Cu(111) surfaces and its effect on the oxidation of copper were investigated using ultra-high vacuum (UHV) spectroscopic techniques. The results were compared to those obtained for ULP deposition on the oxide-covered Cu(111) surface prepared in air. The thermal stability of the adsorbed molecular layer under UHV was also studied. This work brings new insight into the interaction of 2-MBT with copper, which allow us to better understand its corrosion inhibition mechanisms.

2. Material and methods

A high purity (99.999%) Cu(111) single-crystal was used in this work. The surface was mechanically polished to 1/4 μm (diamond paste), successively rinsed with acetone, ethanol, and ultra pure (UP) water (resistivity $>$ 18 MΩ·cm), and then electropolished in 60 wt%

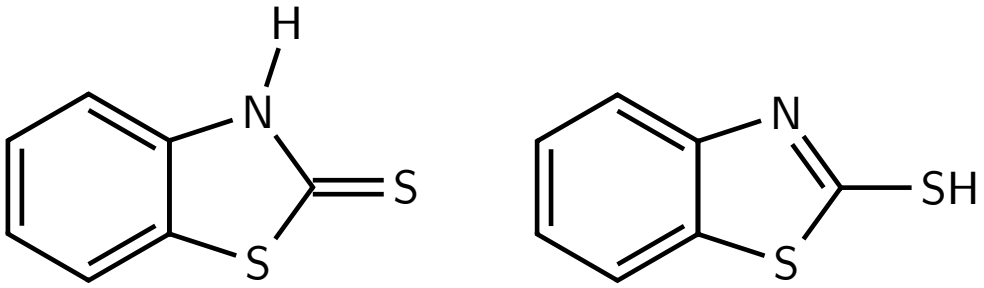

Figure 1: Thione form (left) and thiol form (right) of 2-MBT.

H_3PO_4 solution at 1.4 V during 5 min, followed by rinsing with 10 wt% H_3PO_4 solution and UP water before introduction in UHV.

For ULP exposure on metallic Cu(111), the sample was further prepared in a UHV platform equipped with X-ray photoelectron spectroscopy (XPS, Thermo Electron Corporation, ESCALAB 250) with base pressure of $\sim 10^{-10}$ mbar. UHV sample preparation was performed by Ar^+ ion sputtering ($P_{Ar} = 5 \times 10^{-6}$ mbar, 600 V, 10 mA, 10 min) followed by 10 min of annealing at 600°C. Sputtering/annealing cycles were repeated until a clean surface was obtained with no contamination detected in the XPS survey spectrum and a sharp (1×1) LEED pattern.

2-MBT with chemical formula $C_7H_5NS_2$ exists in two forms as shown in Fig. 1, with thione form prevailing in solid and gas phase [28]. A reactor for molecular deposition is connected to the preparation chamber of the UHV platform. 2-MBT yellow powder (Sigma-Aldrich) with purity of 99% was placed in a vacuum sealed glass tube connected directly to the reactor. The tube was kept at room temperature, and the partial pressure of 2-MBT was 2×10^{-9} mbar. The molecular exposure was calculated by multiplying the pressure of 2-MBT by the dosing time (1 L = 10^{-6} torr s). The sample was exposed to 2-MBT vapour at room temperature, and the surface after exposure was analysed by XPS.

A monochromatic Al K_α source (1486.6 eV) was used and the binding energy was referenced by measuring the Fermi level position of the sample. The transmission of analyser was calibrated by measurement of reference samples. The survey spectrum was recorded with a

pass energy of 100 eV corresponding to an overall resolution of 1.8 eV, the high resolution spectra were recorded with a pass energy of 20 eV corresponding to an overall resolution of 360 meV. The take-off angle of the analysed photoelectrons was 90° for all analyses except when mentioned. The data processing was carried out using the CasaXPS software (version 2.3.19) [29].

In order to investigate the influence of pre-oxidation on the adsorption of 2-MBT, the ULP dosing experiments were carried out on a pre-oxidized copper surface prepared by introducing oxygen in the main chamber via a leak valve (5×10^{-6} mbar) until saturation at room temperature. In this case, a 2D oxide layer is formed [30]. ULP exposure was also carried out on Cu(111) surface prepared in air as described above without further preparation under UHV in order to study the influence of a native 3D oxide layer on the interaction mechanism of 2-MBT. Finally, the oxidation of a surface covered by a 2-MBT film was investigated by Auger electron spectroscopy (AES, Omicron model CMA-100) in order to determine the inhibition capacity of the 2-MBT films.

3. Results and discussion

3.1. Bare Cu(111) exposed to 2-MBT and thermal stability of adsorbed multilayer

The growth kinetics of 2-MBT on clean, metallic Cu(111) at ULP (2×10^{-9} mbar) and room temperature was followed by XPS. The area of the S 2p, C 1s and N 1s core level peaks were normalized by the transmission of analyser, the photoionization cross section and the inelastic mean free path. The normalized peak area is proportional to the density of atoms. Fig. 2 shows the change in the XPS normalized area of the S 2p, C 1s and N 1s core level peaks as a function of exposure to 2-MBT. Lines showing the evolution of different signals are added to guide the reader's eye.

Fast increases of the S 2p, C 1s and N 1s signals with exposure are observed, indicating the deposition of 2-MBT on the sample surface, followed by a decrease in the adsorption rate until saturation of the measured signals for an exposure of about 90 L. The atomic ratios of S and N versus C were calculated, and we obtain a N to C atomic ratio of 0.10 ±

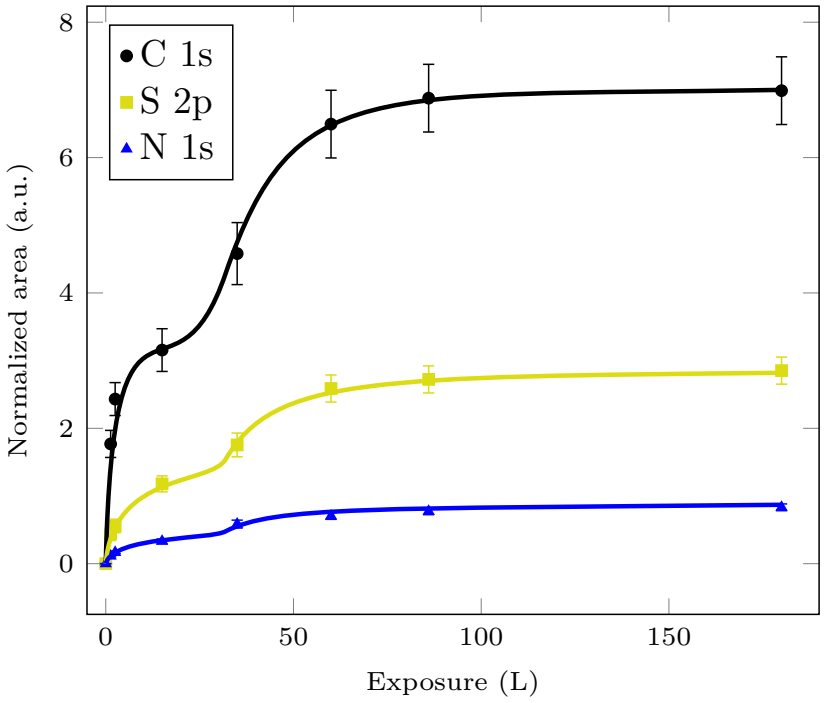

Figure 2: Growth kinetics of 2-MBT on clean Cu(111) surface at RT. Change in the XPS normalized area of the S 2p, C 1s and N 1s core level peaks as a function of 2-MBT exposure at 2×10^{-9} mbar. Lines are added to guide reader's eye.

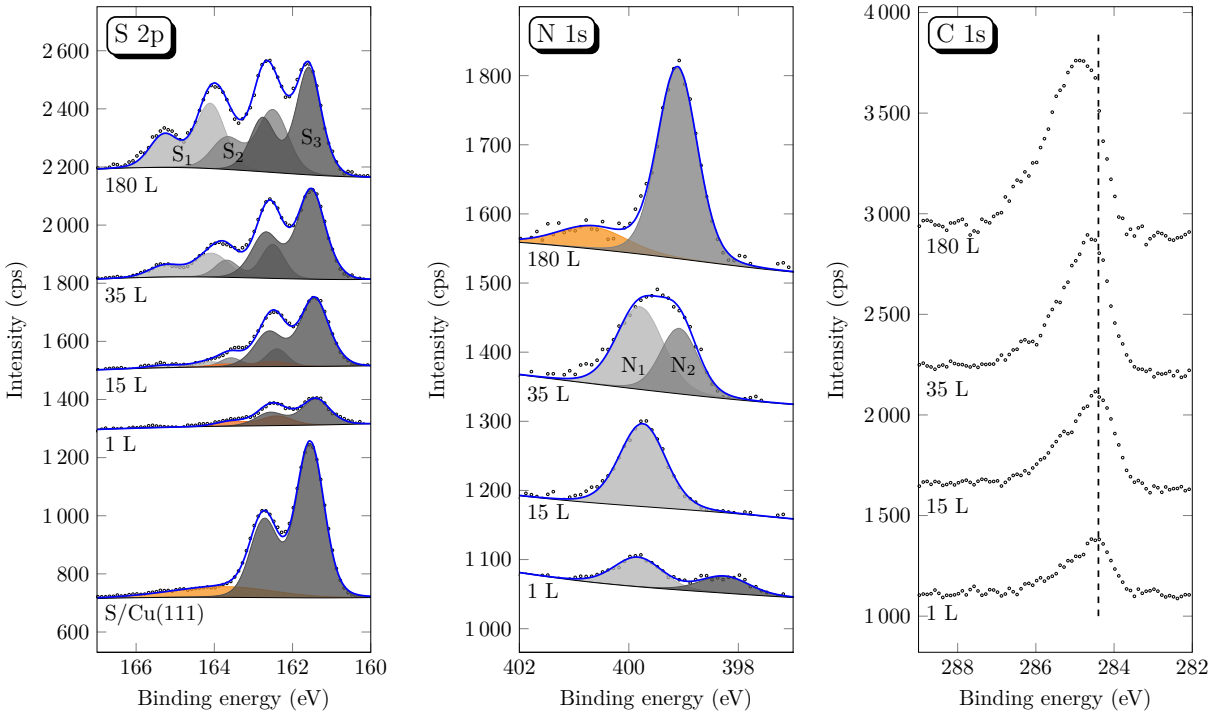

Figure 3: XPS spectra of the S 2p, N 1s and C 1s core levels after 2-MBT exposure on metallic Cu(111) surface at 2×10^{-9} mbar and RT. S 2p spectrum for a $(\sqrt{7} \times \sqrt{7})$R19.1° S/Cu(111) surface is shown for comparison.

0.01, which is similar to the theoretical value for the stoichiometry of the molecule (1/7). The slight difference could be explained by possible geometric effects. The S to C atomic ratio was calculated to be 0.42 ± 0.01, which is 1.5 times the theoretical value (2/7).

In order to explain this excess of S, a detailed high resolution XPS analysis of the molecular layers formed after different exposures was performed in order to determine their chemical composition. The results are shown in Fig. 3. The S 2p spectra were decomposed using spin-orbit doublets S $2p_{1/2}$ and S $2p_{3/2}$, with a branching ratio of 0.5 and spin-orbit splitting of 1.18 eV [24, 26]. At low exposure, i.e. 1 L, the S 2p spectrum is mainly composed of one S_3 component, with the $2p_{3/2}$ at 161.4 eV. This peak is at the same position as that of the $(\sqrt{7} \times \sqrt{7})$R19.1° S/Cu(111) surface obtained by exposing clean Cu(111) surface to H_2S, suggesting a partial decomposition of 2-MBT by the cleavage of the C=S and C–S bonds when interacting with metallic copper, and the adsorption of atomic S, as also confirmed

by STM [31]. This phenomenon could be explained by the high affinity of sulfur to copper [32–36]. Moreover, angle resolved measurements confirm that S_3 is a component at the interface. The S_3 component is thus attributed to S bonded to metallic copper.

At higher exposure (15 L), besides the increase of S_3 component, two other components S_1 and S_2 appear, with the $2p_{3/2}$ at 164.1 eV and 162.5 eV, corresponding to the endocyclic and exocyclic S atoms in the 2-MBT molecule, respectively [24, 37]. The intensities of S_1 and S_2 components were set to be the same, their full widths at half maximum (FWHM) were limited to 1.0 eV, and the fit is in good agreement with the measured XPS spectra. The appearance of S_1 and S_2 indicates the formation of a molecular layer above the layer directly bonded to metallic copper, which is in agreement with the formation of a full monolayer at 10 L observed by STM [31]. Further exposure to 2-MBT results in an increase of S_1 and S_2, indicating a multilayer growth on Cu(111) surface.

A transition of N 1s spectra from N_1 (399.8 eV) to N_2 (399.1 eV) was observed, N_2 is assigned to N in non bonded molecule. As for N_1, two possibilities exist to explain the shift of 0.7 eV in binding energy. N may bond directly to copper at the interface, or, since S is bonded to copper, it may change the electronic density of other elements in the molecule. The presence of N_1 component suggests the adsorption of 2-MBT on copper in its molecular form, thus the S_3 component should be considered as the sum of the components corresponding to S bonded to Cu, i.e. atomic S (resulting from the molecule decomposition) and S in the molecule. The binding energies of molecular and atomic S interacting with metallic copper being too close to be distinguished. Moreover, the two S atoms are both bonded to Cu in the molecular form, as indicated by a good fit with one S_3 component and two identical components S_1 and S_2. A shift to higher binding energy until 0.4 eV in C 1s region was observed. Due to low signal-to-noise ratio and non-obvious peak separation, as well as the direct interaction of 2-MBT with copper, the decomposition of C 1s region can not give reliable information and is thus not performed.

We can follow the evolution of different S and N components with exposure, as shown in Fig. 4. Smooth lines allowing to better follow the evolution of different components are added. The XPS peak area is normalized as in Fig. 2 to be proportional to the density of

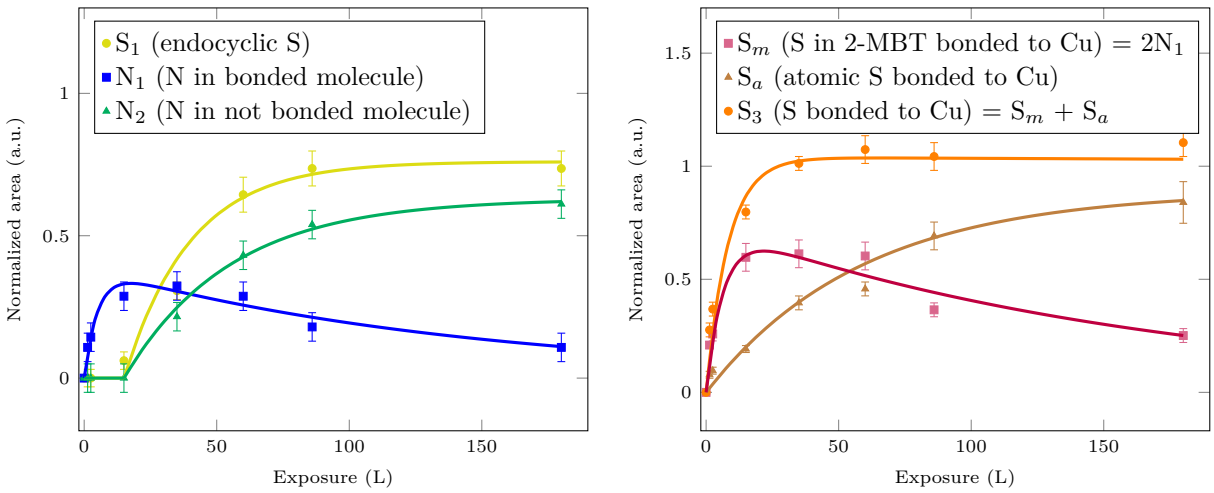

Figure 4: Evolution of the different S and N components with exposure to 2-MBT. Lines are added to guide reader's eye.

atoms. The relative components associated to atomic (S_a) and molecular S (S_m) in S_3 can be disentangled by imposing the atomic ratio between S_m and N_1. Firstly, we observe an increase of N_1 and S_m followed by a slow decrease, with maximum value at around 15 L. The absence of S_1 and N_2 during the initial stage indicates the formation of a first monolayer which becomes complete at around 15 L. After 15 L, S_1 and N_2 begin to appear, indicating the formation of 2-MBT multilayer. Finally a stationary regime is reached. S_a is found to increase continuously with increasing exposure, which may be explained by a further decomposition and a possible densification of the monolayer at higher exposure.

In order to better understand the interaction of 2-MBT with copper, exposure was also carried out in the same conditions on Cu(111) prepared in air, and the results are shown in Fig. 5. In this case, a 3D oxide formed in air is covering the Cu(111) surface before 2-MBT deposition, and the presence of S 2p, N 1s and C 1s signals indicates the adsorption of the molecule. However, the S 2p spectrum shows only two components S_1 and S_2 corresponding to S in molecules which are not bonded to copper. This confirms that S_3 component is effectively associated to S bonded to metallic Cu. The pre-adsorbed 3D oxide prevents the direct interaction with metallic Cu and the dissociation of the molecule.

The high signal-to-noise ratio and the absence of direct molecule/copper interaction

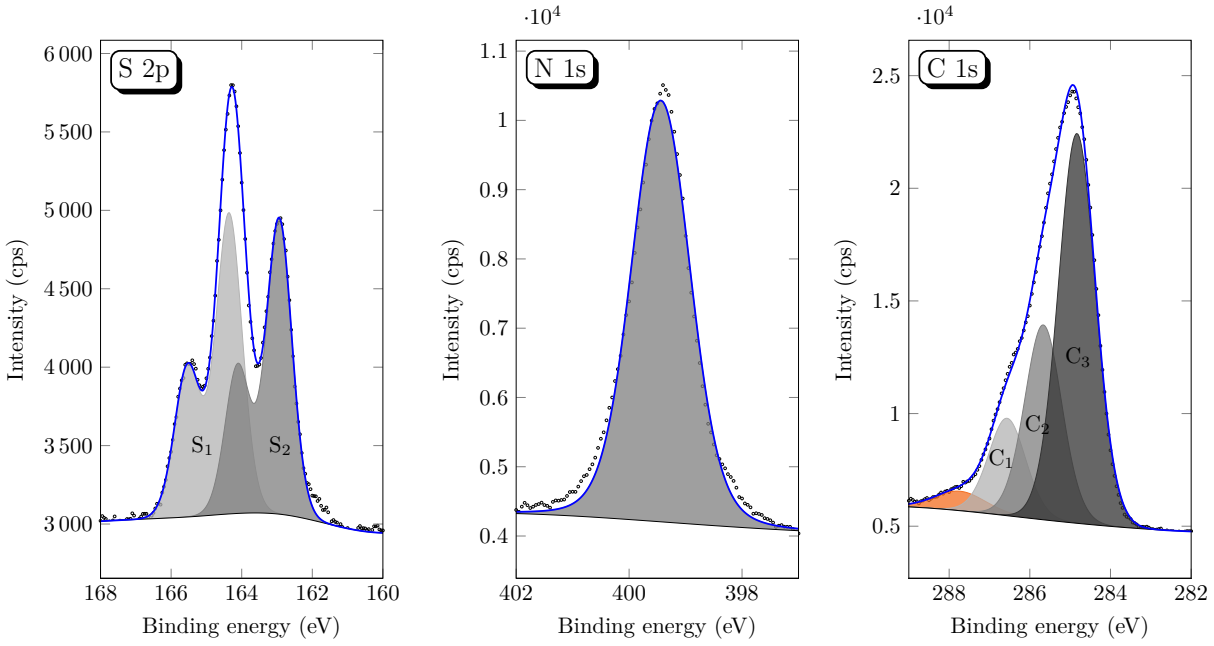

Figure 5: XPS spectra of the S 2p, N 1s and C 1s core levels after exposures to 2-MBT at ULP (180 L) and RT on Cu(111) prepared in air.

allow the decomposition of the C 1s region. There are theoretically seven inequivalent carbon environments within the molecule, however, XPS may not distinguish between the four benzene-like carbon atoms not in direct contact with N or S [38, 39]. We assume thus mainly three types of carbon, C_1, C_2 and C_3. The FWHMs (1.0 eV) of these three components were set to be the same, the intensity of C_1 was set to be half of C_2, which itself was half of C_3, and the fit is in agreement with the measured spectrum. We obtain three components at binding energies of 284.8 eV, 285.6 eV and 286.6 eV for C_3, C_2 and C_1, respectively. C_1 is then assigned to C=S, C_2 to C–N and C–S, and C_3 represents the remaining C atoms in the benzene ring. The good fit with the experimental data confirms non-dissociative molecular adsorption on the surface pre-covered by a 3D oxide layer. In the case of exposure on metallic Cu(111) prepared under UHV (Fig. 3, 180 L), a slight shift of 0.1 eV to lower binding energy of C 1s spectrum is observed, indicating a change in the C bonding in the molecule interacting with metallic copper. The same phenomenon is observed for the N 1s region, with a shift of 0.3 eV to lower binding energy and a decrease in

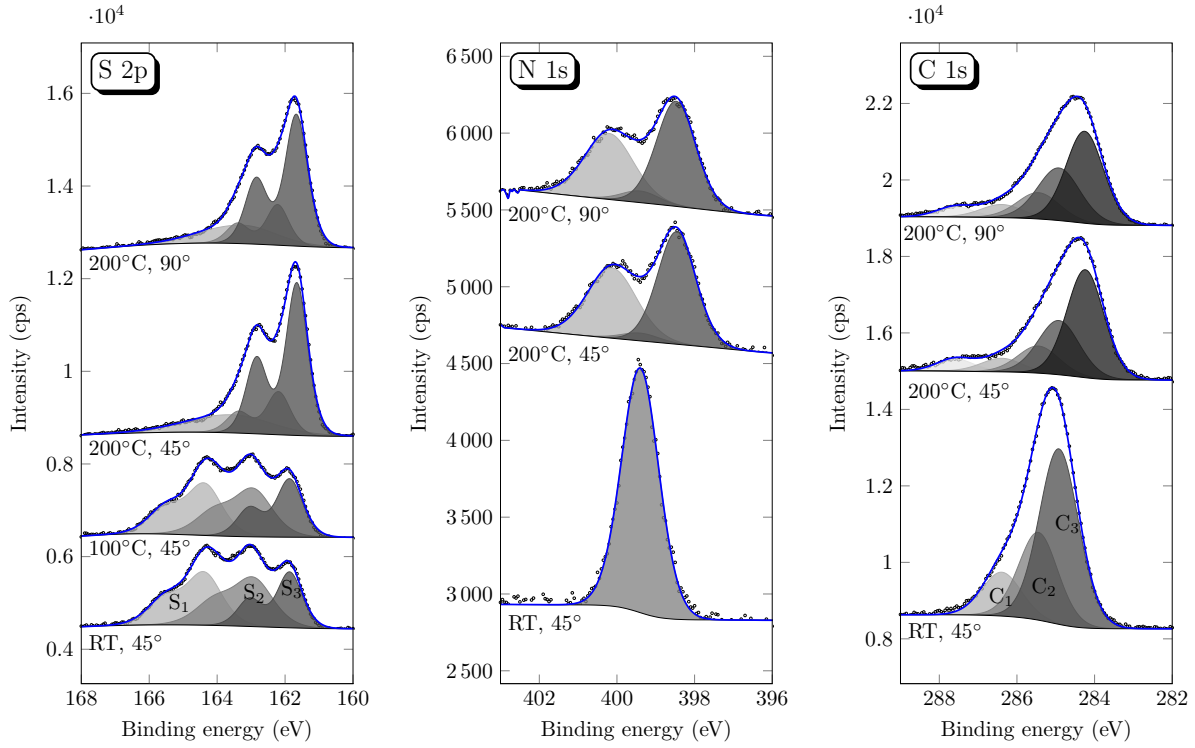

Figure 6: XPS spectra of the S 2p, N 1s and C 1s core levels for Cu(111) saturated with 2-MBT (ULP) before and after annealing during 20 min (take-off angle: 45° or 90° as indicated).

FWHM (0.9 eV) of about 25%. The increase in FWHM and the small deviations in the fit of S 2p and N 1s spectra for exposure on Cu(111) prepared in air may be explained by the presence of surface contaminations when exposed to air. The C 1s component at binding energy of 287.7 eV is assigned to carboxylic groups (air contamination) [40].

In order to examine the thermal stability of the 2-MBT layer deposited under ULP conditions on oxide-free Cu(111), annealing at different temperatures during 20 min was carried out on saturated surfaces. XPS analyses performed before and after annealing are shown in Fig. 6. Firstly, XPS spectra were recorded at a take-off angle of 45°. After annealing at 100°C, the S 2p spectrum shows almost no change. We find the three S components associated to sulphur in non bonded molecule (S_1 and S_2) and sulphur interacting with metallic copper (S_3), with almost the same intensity and FWHM compared to those obtained before annealing. In contrast, when the sample was heated to 200°C, the total intensity of

S increased by 8%, and the fraction of S_3 was twice that before annealing, while that of molecular S (S_1 and S_2) was reduced by half. The relative proportion of molecular C was reduced to half, and that of molecular N strongly decreased, with appearance of other C and N components at lower and higher binding energies, suggesting decomposition of 2-MBT. At the same time, the total intensity of C decreased by about 30%, and that of N decreased by 17%, indicating the partial desorption of the molecular layer. This dissociative desorption of the molecular layer contributes to the increase of the remaining S component associated to S bonded to Cu(111) through a reduced attenuation of the signal.

In order to determine any stratification of the molecular layer after annealing, XPS measurements were also carried out in more sub-surface-sensitive conditions, at a take-off angle of 90° (Fig. 6). Compared to the spectra obtained at 45°, the relative proportion of S_3 versus molecular S (S_1 and S_2) increased slightly, as well as the relative proportion of molecular C and N versus that of C and N after molecule decomposition. This seems to indicate that the surface is firstly covered by sulphur, followed by the 2-MBT molecule, and finally by decomposition products (C and N).

3.2. Pre-oxidized Cu(111) exposed to 2-MBT and thermal stability of adsorbed multilayer

In order to study the influence of surface oxidation on the adsorption of 2-MBT, the Cu(111) surface was pre-oxidized ($P_{O_2} = 5 \times 10^{-6}$ mbar, 15 min, RT), and exposure of 2-MBT was then performed at room temperature under ULP at $2{\times}10^{-9}$ mbar. The conditions of pre-oxidation were selected so as to saturate the surface with a 2D oxide layer [30].

Fig. 7 shows the variation of the XPS normalized area of the S 2p, C 1s, N 1s and O 1s core level peaks with 2-MBT exposure. The XPS peak area is normalized similarly as above to be proportional to the density of atoms, and lines showing the evolution of different signals are added to guide the reader's eye. A rapid increase of the S 2p, C 1s and N 1s signals is observed, indicating the growth of 2-MBT on the pre-oxidized copper surface. It is important to notice that the growth of 2-MBT layer is accompanied by a continuous decrease of the oxygen signal. Oxygen is substituted by 2-MBT with dissociation of the initial 2D oxide layer, and it may desorb as gaseous O_2 [41, 42]. The results are in agreement with

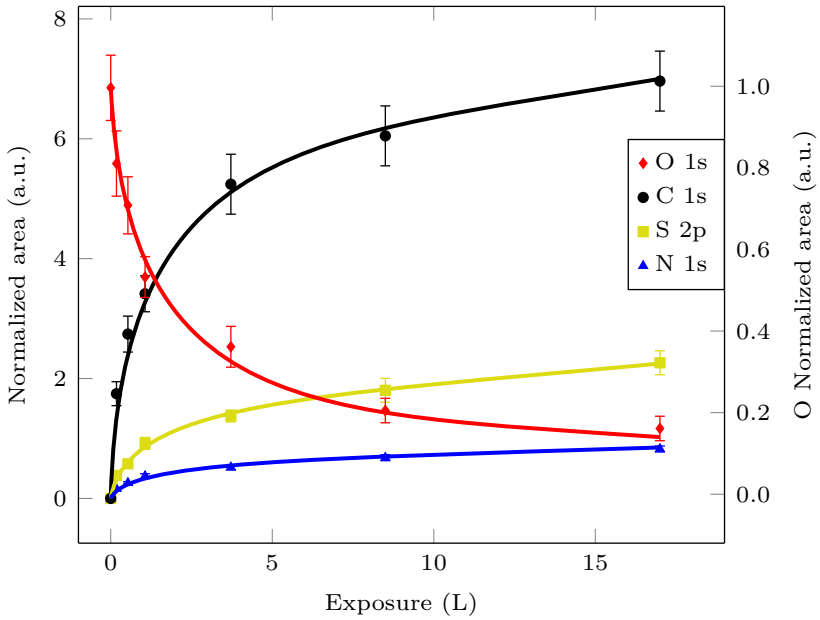

Figure 7: Growth kinetics of 2-MBT on pre-oxidized Cu(111) at RT. Changes in XPS normalized area of the S 2p, C 1s, N 1s and O 1s core level peaks as a function of 2-MBT exposure at 2×10^{-9} mbar. Lines are added to guide reader's eye.

that obtained by AES [31], where a complete disappearance of oxygen was observed after about 25 L. The atomic ratios of S and N versus C were calculated, we obtain values close to the stoichiometry of the molecule, indicating the adsorption of 2-MBT in its molecular form on the pre-oxidized Cu(111) surface.

Similarly, a high resolution XPS analysis of the molecular layer formed on pre-oxidized Cu(111) after different exposures was performed, and the results are shown in Fig. 8. At low exposure (0.2 L), the S 2p region is mainly composed of S_3 component at 161.6 eV, and a decrease in the O 1s spectrum of 19% compared to that obtained before exposure is observed, indicating the substitution of oxygen by 2-MBT and direct bonding between S and Cu. The N 1s spectrum gives a component N_3 at 398.3 eV, which is assigned to N in the bonded molecule. At an exposure of 0.5 L, we observe an increase of S_3 component and the appearance of two other components S_1 and S_2 corresponding to S in non bonded 2-MBT. Moreover, the N_2 component at 399.0 eV representing N in non bonded molecule begins to appear. This seems to indicate the formation of a second layer from 0.5 L. The presence

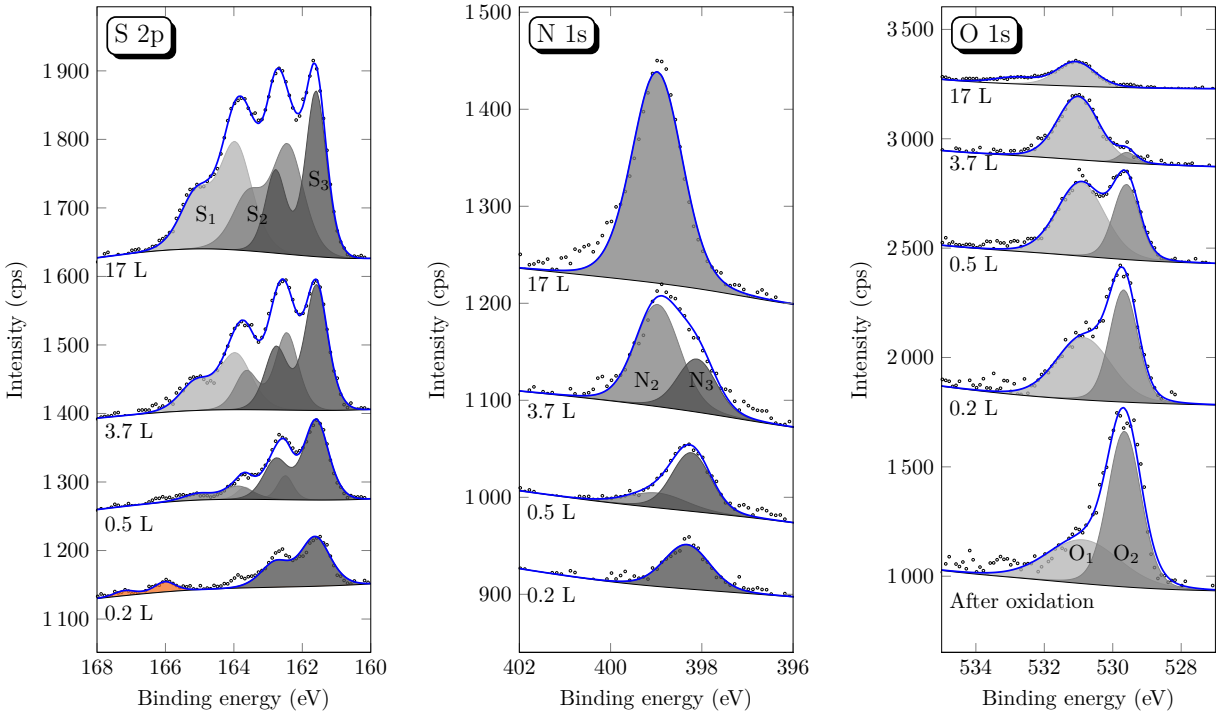

Figure 8: XPS spectra of the S 2p, N 1s and O 1s core levels after 2-MBT exposure on pre-oxidized Cu(111) surface at 2×10^{-9} mbar and RT.

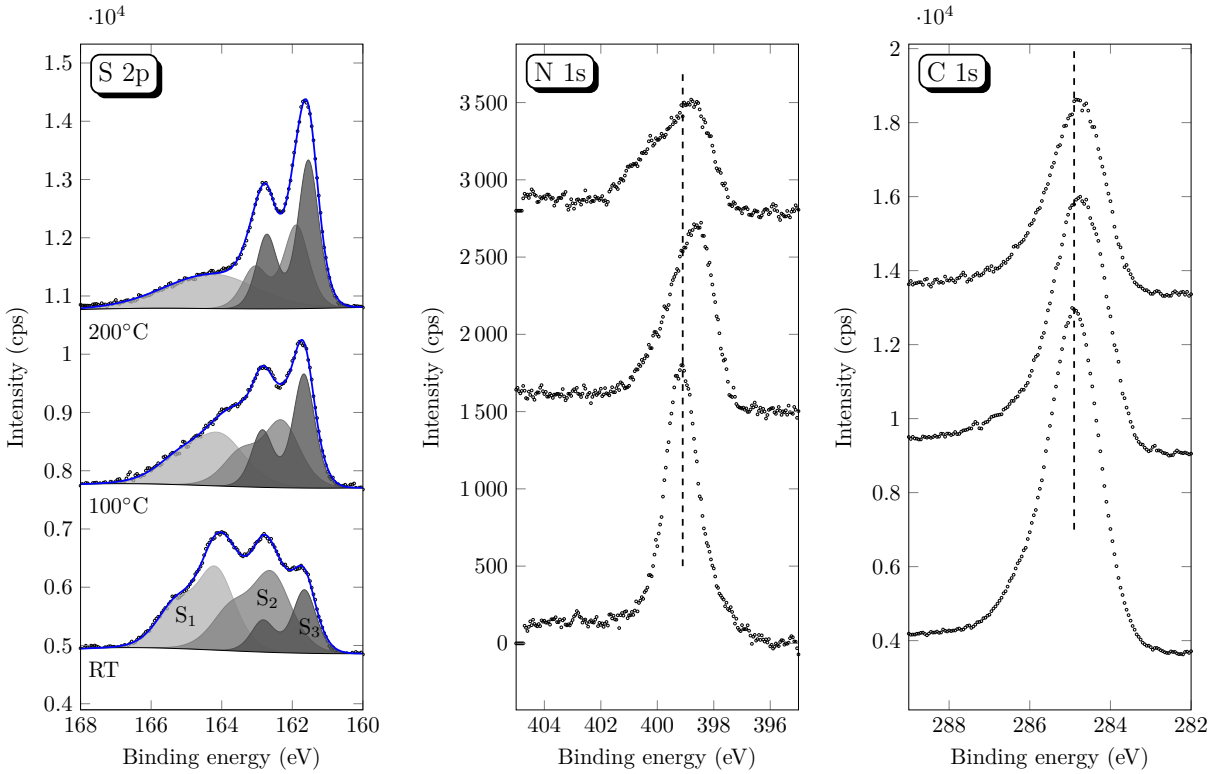

Figure 9: XPS spectra of S 2p, C 1s and N 1s core levels for pre-oxidized Cu(111) saturated with 2-MBT (ULP) before and after annealing during 20 min (take-off angle: 45°).

of O 1s signal at 0.5 L indicates that the surface is partially covered by 2-MBT molecular layer where oxygen has been substituted. Compared to the spectra obtained for adsorption of 2-MBT on the clean metallic copper surface, a difference of 1.5 eV towards lower binding energy from N_1 to N_3 is observed, indicating a stronger interaction of N with metallic Cu, which may be assigned to direct bonding between N and Cu. This explains the slight shift of the S_3 component. Further exposure to 2-MBT leads to the growth of molecular layer as indicated by the increase of S_1 and S_2 components, and continuous decrease of O 1s spectra.

In order to assess the thermal stability of the 2-MBT layer formed on pre-oxidized surface, annealing at different temperatures was carried out (Fig. 9). Decomposition and partial desorption of the molecule were observed when the sample was heated above 100°C, as shown by an increase of the relative proportion of S_3 component and a decrease of intensities of C 1s and N 1s, as well as a shift to lower binding energy of the XPS spectra. However,

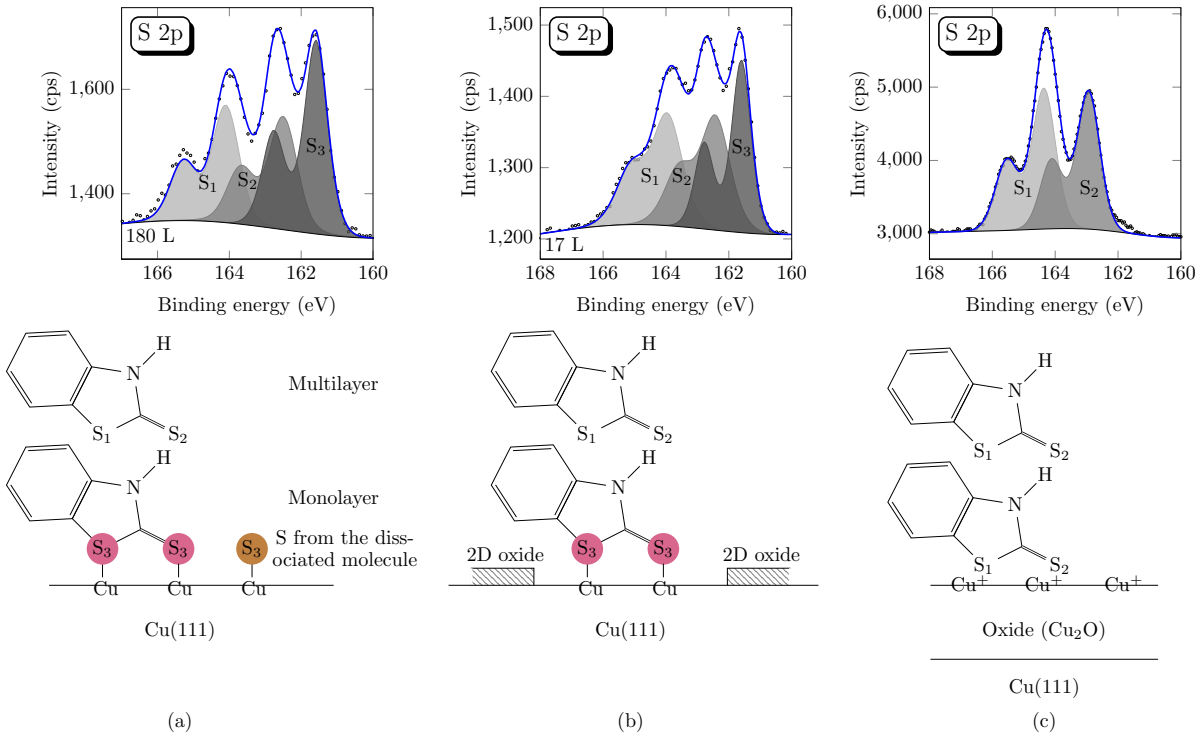

Figure 10: Schematic illustration of 2-MBT adsorption on different copper surfaces and the corresponding chemical state of S measured by XPS: (a) metallic; (b) oxidized (2D oxide); (c) oxidized (3D oxide).

compared to annealing of adsorbed molecular layer on metallic Cu(111), difference in the N 1s region can be observed, with non-obvious peak separation, which may be explained by the bonding between N and Cu for exposure on metallic Cu(111). A schematic illustration of the adsorption of 2-MBT on clean and pre-oxidized Cu(111) surfaces is summarized in Fig.10. The inclination angle between the molecule and the sample surface is not considered.

3.3. Thickness of the 2-MBT layers

Quantitative analysis of the XPS data was performed in order to determine the thickness of the molecular layers (d_{MBT}) formed at ULP on metallic and pre-oxidized Cu(111) surfaces. We assume that the sample surface was covered by a homogeneous layer of 2-MBT on metallic Cu(111) surface. In the presence of a 2D oxide, we assume a homogeneous molecular layer on Cu(111) surface where oxide has been replaced by 2-MBT.

The thickness of the inhibitor layer was calculated from the intensities of the S 2p, N 1s,

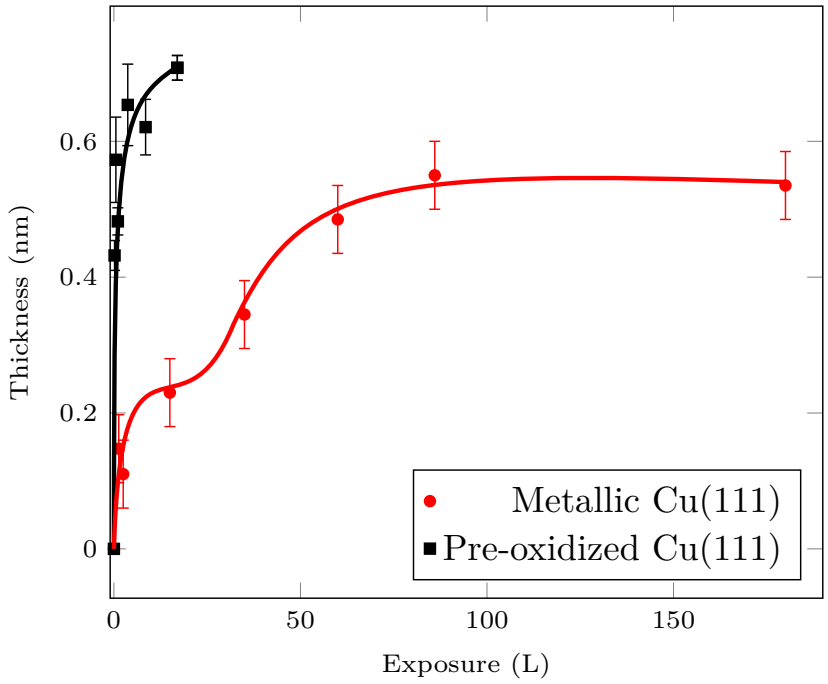

Figure 11: Thickness of the molecular layer formed on metallic and pre-oxidized Cu(111) surfaces. Lines are added to guide reader's eye.

O 1s and Cu 2p spectra, using the following set of equations.

$$I^{\mathrm{MBT}}_{\mathrm{S\ 2p}} = (1-\phi)kFSN^{\mathrm{MBT}}_{\mathrm{S}}\sigma_{\mathrm{S\ 2p}}T_{\mathrm{S\ 2p}}\lambda^{\mathrm{MBT}}_{\mathrm{S\ 2p}}\sin\theta\left[1-\exp\left(-\frac{d_{\mathrm{MBT}}}{\lambda^{\mathrm{MBT}}_{\mathrm{S\ 2p}}\sin\theta}\right)\right] \quad (1)$$

$$I^{\mathrm{MBT}}_{\mathrm{N\ 1s}} = (1-\phi)kFSN^{\mathrm{MBT}}_{\mathrm{N}}\sigma_{\mathrm{N\ 1s}}T_{\mathrm{N\ 1s}}\lambda^{\mathrm{MBT}}_{\mathrm{N\ 1s}}\sin\theta\left[1-\exp\left(-\frac{d_{\mathrm{MBT}}}{\lambda^{\mathrm{MBT}}_{\mathrm{N\ 1s}}\sin\theta}\right)\right] \quad (2)$$

$$I^{\mathrm{Cu}}_{\mathrm{Cu\ 2p}} = (1-\phi)kFSN^{\mathrm{Cu}}_{\mathrm{Cu}}\sigma_{\mathrm{Cu\ 2p}}T_{\mathrm{Cu\ 2p}}\lambda^{\mathrm{Cu}}_{\mathrm{Cu\ 2p}}\sin\theta\exp\left(-\frac{d_{\mathrm{MBT}}}{\lambda^{\mathrm{MBT}}_{\mathrm{Cu\ 2p}}\sin\theta}\right)+\phi I^{\mathrm{Cu(2D\ oxide)}}_{\mathrm{Cu\ 2p}} \quad (3)$$

where I is the intensity of the photoelectrons, ϕ the surface coverage by the 2D oxide, N the density of emitting atoms, λ the inelastic mean free path, estimated using the Tanuma, Powell and Penn formula (TPP-2M) [43], and θ the take-off angle of photoelectrons. $\phi = 0$ for exposure on the metallic Cu(111) surface, and $\phi = I_{\mathrm{O\ 1s}}/I^{\mathrm{2D\ oxide}}_{\mathrm{O\ 1s}}$ for exposure on the pre-oxidized Cu(111) surface.

The results are shown in Fig. 11. Lines are added to show the thickness evolution. Growth of molecular layer is observed with a fast increase of the inhibitor layer thickness

at initial stage, followed by a decrease in the growth rate until saturation for exposure on the metallic Cu(111) surface. Moreover, an acceleration of the initial growth kinetics of 2-MBT is observed in the presence of oxygen, which may be explained by the activation of the molecule bonding to copper by the dissociation of the pre-formed surface oxide.

We concluded above on the formation of a complete monolayer at 15 L on the metallic Cu(111) surface, which corresponds to a thickness of about 0.2 nm. Taking into account the dimension of the 2-MBT molecule [44], we can deduce that 2-MBT in the monolayer adsorbs with its plane almost parallel to the sample surface. This is consistent with the fact that S-containing molecules can adsorb on metallic surface with small tilt angle [45, 46]. Multilayers are formed at higher exposure, with a total thickness of 0.6 nm at saturation. On pre-oxidized Cu(111) surface, the monolayer formed is 0.4 nm after an exposure of 0.2 L, which indicates that the molecule adsorbs in a tilted position. Multilayers of thickness of 0.7 nm are formed at 17 L. For 2-MBT exposure at ULP on Cu(111) prepared in air until saturation, by assuming a homogeneous oxide layer covered by a homogeneous layer of 2-MBT, we can calculate the thickness of oxide and molecular layers, which gives 0.6 $\pm$ 0.1 nm and 1.0 $\pm$ 0.1 nm, respectively. The 2-MBT layer formed on Cu in aqueous solution was reported to be 1.5 $\pm$ 0.5 nm [24]. This indicates that the presence of oxygen prior to exposure can promote the growth of 2-MBT.

3.4. Inhibition effect of pre-adsorbed 2-MBT on oxidation of Cu(111)

In order to confirm if 2-MBT pre-adsorbed under ULP conditions could inhibit copper corrosion, we recorded the oxidation kinetics on the Cu(111) surface first exposed to 8 L of 2-MBT at room temperature, corresponding to the formation of about one monolayer of 2-MBT. Oxidation of the sample was then performed at $P_{O_2} = 5 \times 10^{-6}$ mbar at RT. Fig. 12 shows that in the presence of the pre-adsorbed monolayer of 2-MBT, there is almost no increase in the oxygen intensity, whereas without 2-MBT copper is oxidized and the oxidation kinetics agree with previous reported data [30]: the intensity of oxygen increases with exposure until the formation of a monolayer of oxide, then the surface is saturated with oxygen, with a value of $h_O/h_{Cu} \sim 0.22$ corresponding to the completion of the 2D

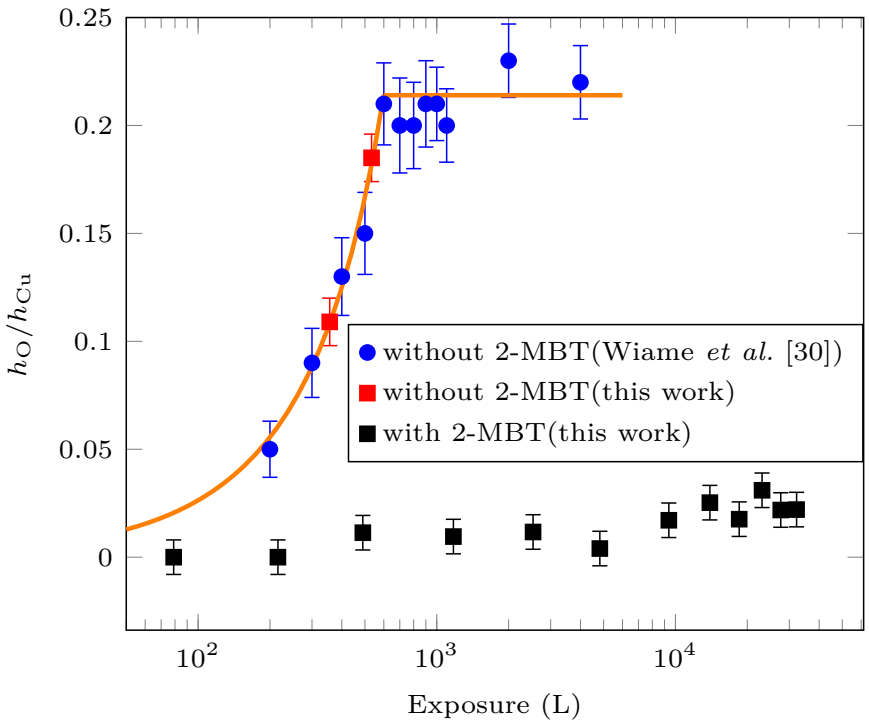

Figure 12: Oxidation kinetics of Cu(111): effect of adsorbed 2-MBT (8 L of 2-MBT at RT prior to oxidation).

oxide layer. The comparison between the oxidation kinetics with and without pre-adsorbed 2-MBT indicates that a monolayer of 2-MBT can effectively protect the copper surface from oxidation in these conditions of temperature and pressure, and thus prevent the formation of copper corrosion products. The residual uptake of oxygen is likely due to the formation of copper oxide at the local sites of the 2-MBT layer where protection is defective. The defective sites cover about 8% of the surface area.

4. Conclusions

In this work, the adsorption of 2-MBT deposited from the vapour phase on metallic and pre-oxidized Cu(111) surfaces under ULP conditions was investigated by XPS. When 2-MBT molecules arrive on a clean metallic copper surface (prepared under UHV), the XPS spectra show that the two sulphur atoms are involved simultaneously in the interaction with copper, confirmed by the presence of a S $2p_{3/2}$ peak at 161.5 $\pm$ 0.1 eV. The adsorption is accompanied by a partial decomposition of the molecule giving atomic sulphur adsorbed on

copper. On the pre-oxidized Cu(111) surface, the 2D oxide initially formed is dissociated and substituted by 2-MBT, without decomposition of the molecule.

A complete monolayer of 2-MBT is formed at an exposures of 15 L on metallic Cu(111) surface, with a thickness of 0.2 nm. This is consistent with the adsorption of flat-lying molecule. Further exposure to 2-MBT leads to the formation of multilayers, with a thickness of 0.6 nm at saturation. On pre-oxidized Cu(111), a monolayer covers partially the surface with a thickness of 0.4 nm, suggesting the adsorption of 2-MBT in a tilted configuration. On the Cu(111) surface covered by a native 3D oxide formed in air, 2-MBT also adsorbs without decomposing and the multilayer is 1.0 nm thick at saturation.

By comparing the growth kinetics of 2-MBT on metallic and pre-oxidized Cu(111) surfaces, we can deduce that the presence of a 2D oxide layer accelerates the initial uptake of 2-MBT on copper ($<$ 20 L), and leads to the formation of a thicker molecular layer. This may be explained by the activation of the molecule bonding to copper by the dissociation of the pre-formed surface oxide and substitution of oxygen by 2-MBT.

After heating metallic and pre-oxidized Cu(111) saturated with 2-MBT to above 100°C, molecules decompose. The C and N resulting from decomposition leave the surface, while the atomic S remains adsorbed on copper.

2-MBT is relatively efficient for corrosion inhibition after adsorption under ULP conditions at room temperature. A monolayer of 2-MBT effectively prevents the oxidation of Cu(111) at low O_2 pressure and room temperature.

5. Acknowledgments

This work was supported by the European Research Council (ERC) under the European Union's Horizon 2020 research and innovation program (ERC Advanced Grant CIMNAS no. 741123). We also thank Région Île-de-France for partial funding of the XPS equipment.

References

[1] M. M. Antonijević, M. B. Petrović Mihajlović, Copper corrosion inhibitors. A review, International Journal of Electrochemical Science 3 (1) (2008) 1–28.

[2] M. B. Petrović Mihajlović, M. M. Antonijević, Copper corrosion inhibitors. period 2008-2014. A review, International Journal of Electrochemical Science 10 (2015) 1027–1053.

[3] F. M. A. Kharafi, N. A. Al-Awadi, I. M. Ghayad, R. M. Abdullah, M. R. Ibrahim, Novel technique for the application of azole corrosion inhibitors on copper surface, Materials Transactions 51 (9) (2010) 1671–1676.

[4] G. Gece, Drugs: A review of promising novel corrosion inhibitors, Corrosion Science 53 (12) (2011) 3873–3898.

[5] A. Fateh, M. Aliofkhazraei, A. R. Rezvanian, Review of corrosive environments for copper and its corrosion inhibitors, Arabian Journal of Chemistry In press (2017) http://dx.doi.org/10.1016/j.arabjc.2017.05.021.

[6] M. M. Antonijević, S. M. Milić, M. B. Petrović, Films formed on copper surface in chloride media in the presence of azoles, Corrosion Science 51 (2009) 1228–1237.

[7] M. Finšgar, I. Milošev, Inhibition of copper corrosion by 1,2,3-benzotriazole: A review, Corrosion Science 52 (2010) 2737–2749.

[8] A. Kokalj, Ab initio modeling of the bonding of benzotriazole corrosion inhibitor to reduced and oxidized copper surfaces, Faraday Discussions 180 (2015) 415–438.

[9] C. Gattinoni, A. Michaelides, Understanding corrosion inhibition with van der Waals DFT methods: the case of benzotriazole, Faraday Discussions 180 (2015) 439–458.

[10] A. Kokalj, S. Peljhan, DFT study of adsorption of benzotriazole on Cu_2O surfaces, The Journal of Physical Chemistry C 119 (21) (2015) 11625–11635.

[11] F. Grillo, D. W. Tee, S. M. Francis, H. Früchtl, N. V. Richardson, Initial stages of benzotriazole adsorption on the Cu(111) surface, Nanoscale 5 (12) (2013) 5269–5273.

[12] F. Grillo, D. W. Tee, S. M. Francis, H. Früchtl, N. V. Richardson, Passivation of copper: Benzotriazole films on Cu(111), The Journal of Physical Chemistry C 118 (16) (2014) 8667–8675.

[13] M. R. Vogt, W. Polewska, O. M. Magnussen, R. J. Behm, In situ STM study of (100) Cu electrodes in sulfuric acid solution in the presence of benzotriazole adsorption, Cu corrosion, and Cu deposition, J. Electrochem. Soc. 144 (5) (1997) 113–116.

[14] M. R. Vogt, R. J. Nichols, O. M. Magnussen, R. J. Behm, Benzotrizole adsorption and inhibition of Cu(100) corrosion in HCl: A combined in situ STM and in situ FTIR spectroscopy study, J. Phys. Chem. B 102 (1998) 5859–5865.

[15] M. Sugimasa, L.-J. Wan, J. Inukai, K. Itaya, Adlayers of benzotriazole on Cu(111), (100), and (111) in $HClO_4$ solution, Journal of the Electrochemical Society 149 (10) (2002) 367–373.

[16] W. Polewska, M. R. Vogt, O. M. Magnussen, R. J. Behm, In situ STM study of Cu(111) surface structure and corrosion in pure and benzotriazole-containing sulfuric acid solution, J. Phys. Chem. B

103 (1999) 10440–10451.

[17] O. M. Magnussen, M. R. Vogt, J. Scherer, R. J. Behm, Double-layer structure, corrosion and corrosion inhibition of copper in aqueous solution, Appl. Phys. A 66 (1998) 447–451.

[18] Y. Jiang, J. B. Adams, D. Sun, Benzotriazole adsorption on Cu_2O(111) surfaces: A first-principles study, Journal of Physical Chemistry B 108 (34) (2004) 12851–12857.

[19] C. W. Yan, H. C. Lin, C. N. Cao, Investigation of inhibition of 2-mercaptobenzoxazole for copper corrosion, Electrochimica Acta 45 (2000) 2815–2821.

[20] J. C. Marconato, L. O. Bulhões, M. L. Temperini, A spectroelectrochemical study of the inhibition of the electrode process on copper by 2-mercaptobenzothiazole in ethanolic solutions, Electrochimica Acta 43 (7) (1998) 771–780.

[21] M. Ohsawa, W. Suëtaka, Spectro-electrochemical studies of the corrosion inhibition of copper by mercaptobenzothiazole, Corrosion Science 19 (7) (1979) 709–722.

[22] D. Chadwick, T. Hashemi, Electron spectroscopy of corrosion inhibitors: Surface film formed by 2-mercaptobenzothiazole and 2-mercaptobenzimidazole on copper, Surface Science 89 (1-3) (1979) 649–659.

[23] R. Woods, G. A. Hope, K. Watling, A SERS spectroelectrochemical investigation of the interaction of 2-mercaptobenzothiazole with copper, silver and gold surfaces, Journal of Applied Electrochemistry 30 (2000) 1209–1222.

[24] M. Finšgar, D. K. Merl, An electrochemical, long-term immersion, and XPS study of 2-mercaptobenzothiazole as a copper corrosion inhibitor in chloride solution, Corrosion Science 83 (2014) 64–175.

[25] J. Jia, A. Giglia, M. F. Carrasco, O. Grizzi, L. Pasquali, V. A. Esaulov, 1,4-benzenedimethanethiol interaction with Au(110), Ag(111), Cu(100) and Cu(111) surfaces: Self-assembly and dissociation processes, J. Phys. Chem. C 118 (46) (2014) 26866–26876.

[26] J. Jia, A. Kara, L. Pasquali, A. Bendounan, F. Sirotti, V. A. Esaulov, On sulfur core level binding energies in thiol self-assembly and alternative adsorption sites: An experimental and theoretical study, J. Chem. Phys. 143 (2015) 104702.

[27] M. Beccari, A. Kanjilal, M. G. Betti, C. Mariani, L. Floreano, A. Cossaro, V. Castro, Characterization of benzenethiolate self-assembled monolayer on Cu(100) by XPS and NEXAFS, Journal of Electron Spectroscopy and Related Phenomena 172 (2009) 64–68.

[28] A. K. Rai, R. Singh, K. Singh, V. Singh, FTIR, Raman spectra and ab initio calculations of 2-mercaptobenzothiazole, Spectrochimica Acta Part A 63 (2006) 483–490.

[29] Casaxps manual 2.3.15, Casa Software Ltd (2009).

[30] F. Wiame, V. Maurice, P. Marcus, Initial stages of oxidation of Cu(111), Surface Science 601 (2007)

1193–1204.

[31] X. C. Wu, F. Wiame, V. Maurice, P. Marcus, Adsorption and thermal stability of 2-mercaptobenzothiazole corrosion inhibitor on metallic and pre-oxidized Cu(111) model surfaces, Accepted by Applied Surface Science.

[32] C. Vericat, M. E. Vela, G. Corthey, E. Pensa, E. Cortes, M. H. Fonticelli, F. Ibanez, G. Benitez, P. Carro, R. C. Salvarezza, Self-assembled monolayers of thiolates on metals: a review article on sulfur-metal chemistry and surface structures, RSC Advances 4 (53) (2014) 27730–27754.

[33] G. Ertl, Reactions at surfaces: from atoms to complexity (nobel lecture), Angewandte Chemie International Edition 47 (19) (2008) 3524–3535.

[34] F. Wiame, V. Maurice, P. Marcus, Reactivity to sulphur of clean and pre-oxidised Cu(111) surfaces, Surface science 600 (18) (2006) 3540–3543.

[35] H. Keller, P. Simak, W. Schrepp, J. Dembowski, Surface chemistry of thiols on copper: an efficient way of producing multilayers, Thin Solid Films 244 (1-2) (1994) 799–805.

[36] R. M. Issa, M. K. Awad, F. M. Atlam, Quantum chemical studies on the inhibition of corrosion of copper surface by substituted uracils, Applied Surface Science 255 (5) (2008) 2433–2441.

[37] Y. S. Tan, M. P. Srinivasan, S. O. Pehkonen, S. Y. M. Chooi, Self-assembled organic thin films on electroplated copper for prevention of corrosion, Journal of Vacuum Science & Technology A 22 (4) (2004) 1917–1925.

[38] C. M. Whelan, M. R. Smyth, C. J. Barnes, N. M. D. Brown, C. A. Anderson, An XPS study of heterocyclic thiol self-assembly on Au(111), Appl. Surf. Sci. 134 (1998) 144–158.

[39] C. M. Whelan, M. R. Smyth, C. J. Barnes, HREELS, XPS, and electrochemical study of benzenethiol adsorption on Au(111), Langmuir 15 (1999) 116–126.

[40] M. Finšgar, 2-mercaptobenzimidazole as a copper corrosion inhibitor: Part ii. surface analysis using x-ray photoelectron spectroscopy, Corrosion Science 72 (2010) 90–98.

[41] N. Petrova, I. Yakovkin, Mechanism of associative oxygen desorption from Pt(111) surface, The European Physical Journal B 58 (3) (2007) 257–262.

[42] D. B. Rao, K. Heinemann, D. Douglass, Oxide removal and desorption of oxygen from partly oxidized thin films of copper at low pressures, Oxidation of Metals 10 (4) (1976) 227–238.

[43] S. Tanuma, C. J. Powell, D. R. Penn, Calculations of electron inelastic mean free paths . ix . Data for 41 elemental solids over the 50 eV to 30 keV range, Surface and Interface Analysis 43 (2011) 689–713.

[44] J. P. Chesick, J. Donohue, The molecular and crystal structure of 2-mercaptobenzothiazole, Acta Crystallographica Section B 27 (7) (1971) 1441–1444.

[45] M. Zharnikov, M. Grunze, Spectroscopic characterization of thiol-derived self-assembling monolayers, Journal of Physics: Condensed Matter 13 (49) (2001) 11333.

[46] F. Eberle, M. Metzler, D. M. Kolb, M. Saitner, P. Wagner, H.-G. Boyen, Metallization of ultra-thin, non-thiol SAMs with flat-lying molecular units: Pd on 1, 4-Dicyanobenzene, ChemPhysChem 11 (13) (2010) 2951–2956.